NISTIR 5798

NASA FIRE DETECTION STUDY

William D. Davis and Kathy A. Notarianni
Building and Fire Research Laboratory
National Institute of Standards and Technology

March 1996

U.S. Department of Commerce
Michael Kantor, *Secretary*
Technology Administration
Mary L. Good, *Under Secretary for Technology*
National Institute of Standards and Technology
Arati Prabhakar, *Director*

CONTENTS

LIST OF TABLES

LIST OF FIGURES

NASA FIRE DETECTION STUDY

William D. Davis
Kathy A. Notarianni

ABSTRACT

The National Aeronautics and Space Administration, together with the National Institute of Standards and Technology are in the third year of a five year project designed to set guidelines for fire protection in high bay facilities. A high bay facility is defined in this study as any space with a ceiling height in excess of 18 m. NASA has numerous high bay spaces that are used to perform a variety of functions. A survey of NASA high bay spaces was conducted to determine the number of spaces, the use of the space, fire detection and suppression present, geometry and presence of forced air flow or clean room conditions, and special hazards which would pose substantial fire risks. Based on the survey results, a modeling program was designed which would analyze both specific and generic high bay spaces representative of the NASA inventory. The computation fluid dynamics model **HARWELL-FLOW3D** was used for the modeling. The object of the modeling was to simulate the response of smoke, fusible link, heat, UV/IR, and obscuration detectors to several standard fire scenarios. The modeling was done for both forced air flow and no air flow present in the space. Results of the predicted detector activation times are presented as a function of fire size, ceiling height, and forced air flow.

1 INTRODUCTION

A study of fire detection methods for use by NASA in protecting their high bay structures is presented. A high bay structure is defined in this study as a structure having a ceiling height in excess of 18 m (60 ft). NASA has numerous high bay spaces that are used to perform a variety of mission critical functions. These include structures with ceiling heights ranging from 18.3 m (60 ft) to over 152 m (500 ft), structures containing complex work stands, and structures with interior conditions ranging from class 100 clean rooms with forced ventilation to ordinary aircraft hangars. Fuel loads are also quite diverse with some structures containing very small fuel loads while other structures are involved in shuttle and payload fueling which can include significant amounts of hypergolic fuels.

The analysis conducted in this study dealt with prediction of the expected performance of heat, smoke, and radiation detection systems for simulated fires of the type expected in NASA high bay facilities. The expected performance of smoke, heat, and radiation detectors in simulated fires is calculated using computer modeling. The results of this analysis will aid the development of fire detection strategies for high bay spaces.

2 THE NASA INVENTORY OF HIGH BAY FACILITIES

A survey of NASA high bay facilities was conducted during 1994 to identify the number and size of existing high bay facilities, their usage, and criticality to the NASA mission. The survey identified special hazards, target fire sizes, existing detection and suppression systems, and the presence of forced air flows.

Seventy spaces were identified which had ceiling heights of at least 18 m (60 ft). About half of these spaces had ceiling heights between 18 m and 26 m (60 ft and 85 ft), 36% were between 27 m and 36 m (90 ft and 120 ft) and 13% were in excess of 36 m (120 ft).

Structure types ranged from class 100 clean rooms with flat roofs and forced air flows with velocities up to 1 m/s to aircraft hangars with curved roofs and no forced air flow. Two different forced air flow patterns are used for the clean rooms in the NASA inventory. For the class 100 clean room at Goddard Space Center, air is introduced through supplies that are uniformly spaced across one wall and exits through returns at the opposite wall. All other NASA clean rooms introduce the air through ceiling supplies with air returns positioned on walls near the floor.

The survey dealt with possible fire scenarios in the following manner. The fire protection engineer at the facility was asked to identify the fire scenario of greatest concern in each high bay space as well as the most likely fire scenario to occur. Also requested was information on materials requiring special consideration such as explosive or radioactive materials. An estimate of the maximum acceptable fire size, defined as the largest fire size tolerable in the space, considering the dollar value loss potential and criticality to the NASA mission, was also requested. Guidelines for the maximum acceptable fire size included: 50 kW (e.g., a wastebasket fire), 1 MW (e.g., a 1.5 m^2 floor area of 4.6 m high storage of ordinary combustibles), or greater than 1 MW (e.g., > 0.8 m diameter JP-4 fire).

Survey results gave 39% of the structures having maximum acceptable fire size of less than 50 kW and 9% of the structures having maximum acceptable fire sizes in excess of 1 MW.

The survey requested information on the presence of automatic smoke detectors such as photoelectric, ionization, beam, and/or continuous sampling, and heat detectors such as fixed temperature, rate of rise, or combination, and infrared or ultraviolet flame detectors. For the spaces with heights between 18 and 26 m, (60 and 85 ft), 25% had no detectors, 39% had thermal/smoke detectors with no forced air flow, 22% had thermal/smoke detectors with forced air flow, and 14% had radiation detectors. For the spaces with heights between 27 and 37 m (90 and 120 ft), 32% had no detectors, 32% had thermal/smoke detectors with no forced air flow, 4% had thermal/smoke detectors with forced air flow, and 32% had

radiation detectors. For the spaces with heights greater than 37 m (120 ft), 45% had no detectors, 22% had thermal/smoke detectors with forced air flow, and 33% had radiation detectors.

3 FIRE SCENARIOS

Fire sizes used to analyze detector performance are based on the NASA survey results. Fire size categories used in the survey included fires with maximum heat release rates of 50 kW, 1 MW, and greater than 1 MW. Clean room facilities typically required fire detection by the 50 kW fire size while general purpose buildings which contained no explosive fuels generally could tolerate 1 MW or higher fire sizes before fire detection was necessary.

For the purposes of this study, 50 kW, 0.5 MW, 1 MW, 4 MW, and 50 MW fire sizes were chosen for the simulations. The simulated fires were chosen to grow quadratically with time ('t-squared'), with each fire reaching its peak heat release rate in 100 seconds. The 50 kW fire would represent a slow growth rate fire[1] in a situation where the fuel load would be small. The 0.5 MW, 1 MW, and 4 MW fires would represent fast growth rate fires[1], and the 50 MW fire would represent a substantial fuel spill such as a hypergolic fuel with an extremely rapid fire spread.

4 MODELING

The results presented in this paper are based on calculations performed using the computational fluid dynamics model (CFD), HARWELL FLOW3D [2], and the radiation model, RADTECT. The CFD model solves the Navier-Stokes equations in three dimensions to determine the heat transfer and flow fields in an enclosure. For turbulent flow, a k-ε model [3] is used to approximate the effect of turbulence on the flow and heat transfer. The set of coefficients used in these studies was used to simulate a plume above an actual fire experiment in a 30 m (100 ft) high hangar [4] and is given in Appendix A.

The modeling technique used to simulate gas flow was to divide the region of interest into a collection of small rectangular boxes or computational volumes. The conditions in each computational volume are initially ambient. Heat is then released in designated computational volumes over time. The resulting flow or exchange of mass, momentum, and energy between computational volumes is determined so that these three quantities are conserved. The momentum conservation or Navier Stokes equations are equivalent to Newton's second law of motion. The energy conservation equation is equivalent to the first law of thermodynamics. These fluid flow equations are expressed mathematically as a set of simultaneous, non-linear partial differential equations. After being discretized, the resulting finite volume equations are solved

iteratively using a variant of Newton's method for computing coupled non-linear algebraic equations.

For the enclosures studied in this paper the number of computational volumes ranged from 13000 to 49000. The sizes of the computational volumes were varied using geometric progressions such that computational volumes representing the fire and the space near the ceiling where detectors would be placed were of sufficient resolution to provide an adequate representation of the flow field. Typically, the length of a side for the computational volumes representing the fire and the plume above the fire at the ceiling ranged in value between 0.2 m and 0.3 m (0.7 ft and 1.0 ft). Symmetry planes were used to reduce the actual modeled space to either one-half or one-quarter of the actual volume. At the walls, the no-slip boundary condition was used. This means that the flow velocities perpendicular and parallel to the wall were assumed to equal zero at the wall. The default turbulent boundary conditions [2] were used to represent the boundary layer formed at the wall.

Convective energy losses from the gas to the ceiling were included in each calculation but the walls of the enclosure were assumed to be adiabatic. The ceiling was assumed to have the properties of steel, with the constants used for modeling given in Appendix A. The assumption of adiabatic walls should have a negligible effect on the calculations owing to the large spaces modeled, the distance that the fire was located from the walls, and the short time duration for the calculations. To account for radiative losses from the fire, 35 per cent of the heat release rate was assumed lost to the walls and ceiling through radiation.

Forced ventilation was modeled by specifying the gas temperature and flow velocity at each supply. Ventilation returns were modeled assuming the derivative of the velocity at the return was continuous across the exit area.

The modeling of radiation was done using a computer program, RADTECT, which calculates the radiative flux from either a point or a conical fire source to a target of arbitrary surface orientation and distance. The total power radiated by the fire was based on the radiative fraction of the total heat release rate for a given fuel. This power is primarily radiated in the infrared region of the electromagnetic spectrum; hence the program is less useful for UV-type detectors unless the UV flux is known.

4.1 HEAT DETECTION

The application of heat detectors in high bay spaces depends on the rate of fire growth and the minimum detectable fire size. For these spaces, the time for heat to reach ceiling mounted detectors can be appreciable and the final temperature of the ceiling jet can be substantially less than the temperature required to activate the

detector due to the entrainment of ambient air and radiative losses to the surrounding environment. Further complications may occur if the path of the heat and smoke is substantially deflected by large objects. In this instance, the time for detection to occur may be substantial and the detection could occur at a different location at the ceiling than the position directly above the fire source.

The temperature of a fusible link detector, typically associated with sprinkler systems, can be modeled in the following manner:

$$\frac{dT_L}{dt} = \frac{\sqrt{v}}{RTI}(T_g - T_L)$$

where T_L and T_g are the fusible link and gas temperatures, RTI is the response time index of the link, v is the speed of the gas flow over the link and t is time [5]. The CFD model was used to determine the local gas temperature and speed for each computational volume, and the actuation time was targeted at 74 °C (165 °F) and 121 °C (250 °F) for the fusible links.

The performance of rate-of-rise detectors was analyzed using the temperature history of each computational volume. Typically, rate of rise detectors will respond if the gas temperature rises over a given temperature range in a specified period of time. For the purposes of this analysis, rate-of-rise detectors were considered activated if the temperature rose more than 12 °C (22 °F) in 60 seconds.

4.2 SMOKE DETECTION

The use of smoke detectors in high bay spaces depends on ceiling height, fire size, fuel type, and the presence of forced ventilation. The basic criterium to judge the activation of optical smoke detectors is percent obscuration produced by the smoke. Different fuels, as well as whether the fire is flaming or smoldering, will produce different concentrations of smoke [6]. The heat release rates representing fires used for this study can only be attributed to flaming fires.

Smoke detection for this study was modeled using two methods. The first method used the temperature rise of the gas at the location of interest. This method is based on the assumption that the temperature rise of a fire driven flow will be proportional to the smoke concentration in the flow. [7] The gas rising from the fire has a certain temperature and smoke density. This model assumes that both cooling and smoke dilution occur only by the entrainment of cooler air. Thus the proportion of smoke density to flow temperature remains constant. Implicit in this assumption are that energy losses from the gas due to radiation and due to heat convection to surfaces are negligible and that the loss of smoke to

surfaces is negligible. Freely rising plumes or gas flows which move short distances over surfaces should satisfy these requirements once the gas temperature drops to the point that radiation losses from the gas are negligible.

An early effort to determine a correlation between temperature rise (ΔT) and smoke obscuration (OB) used wood crib fires to measure the activation of smoke detectors as a function of temperature for fire driven flows. [8] The results of this study suggested that smoke detectors would alarm at an $OB/\Delta T = 1.2 \times 10^{-3}$ (m °C)$^{-1}$.

In a recent test of the response of smoke detectors to a fire in a hospital room [9], the temperature rise associated with the smoke density required to activate ionization detectors rated at an obscuration of 3.3% m^{-1} (1% ft^{-1}) was approximately 5 °C. The fire used in these tests was produced by burning wood cribs and the ceiling height was 2.44 m (8 ft). While the ceiling height was low compared with the high bay facilities studied here, the ionization detectors in the study were located at several distances from the fire and produced the same temperature/smoke correlation.

A set of fire tests conducted with ionization detectors in a 15 m (50 ft) high structure provided an additional opportunity to experimentally test a temperature/smoke correlation [10]. In these tests, the fire was produced by burning wood cribs and JP5 pools. The ionization detectors used responded to an obscuration of 2.5% m^{-1} and were mounted on the ceiling 3 m (10 ft) from the geometric center of the fire pan. Four detectors were available at these positions for each fire. The ambient temperature ranged from 27 °C to 28 °C (81 °F - 82 °F) during the tests. For the 0.61 by 0.61 by 0.61 m (2 ft by 2 ft by 2 ft) wood crib fire, the average temperature rise for detector activation in the plume was 1.3 °C. For the JP5 fires, a 0.61 m by 0.61 m (2 ft by 2 ft) square pan produced an average temperature rise for detector activation of 4.4 °C, and a 2.0 m (6.6 ft) diameter pan produced an average temperature rise of 7.9 °C. The data sampling time for each of the thermocouples in these experiments was once every four seconds. The larger detector threshold temperature for the 2.0 m diameter pan fire compared with the smaller pans is probably the result of the rapid temperature rise observed in the large pan fire. Averaging the response temperatures for the three fires suggests a temperature rise of 5 °C for ionization detector activation responding to an obscuration of 2.5% m^{-1}.

The 5 °C temperature rise was used in this report to determine ionization detector activation based on the experimental results discussed in the prior paragraph. Use of this value requires that the detectors under consideration respond to an obscuration of 2.5% m^{-1}. For detectors responding to higher values of obscuration, higher temperatures may be required for activation.

The second technique for estimating smoke detector activation was

based on calculated smoke concentration. A scalar variable, equal to the optical density per meter at an arbitrary location in the enclosure divided by the optical density per meter in the fire, was used to estimate the smoke concentration. The value of this variable equals one initially and decreases in response to the dilution effect of the calculated flow field entering new computational volumes. Decreases in smoke concentration due to particle clumping and deposition onto surfaces are not included in the calculation. Since different fuels produce different amounts of smoke, the normalization procedure would allow the calculations to be generalized to a variety of different fuels. Hence a smoky fire might produce a detectable signal when the dilution of the scalar variable was 0.001 while a less smoky fuel would not produce a detectable signal at this level.

In order to clarify the meaning of this variable and provide a methodology for its use, a specific example, using wood cribs, is given. Following reference [6], the following variables are defined:

S = ratio of local optical density per meter to optical density per meter at fire source,
ϵ = smoke conversion factor,
m_s = mass of smoke produced,
m_f = mass of fuel burned,
v_l = local average velocity at fire source,
h = heat of combustion of fuel,
h_r = heat release rate per fuel surface area,
K_m = extinction coefficient / mass,
K_s = optical density per meter near fire surface,
K = local optical density per meter.

The rate at which smoke is produced by the fire is given by

$$\dot{m}_s=\epsilon h_r/h$$

The optical density per meter at the fire source is then obtained by

$$K_s=K_m\frac{\dot{m}_s}{v_L}$$

The local optical density per meter is then found from

$$K=K_sS$$

The value of the variable S is found using the CFD calculation, where S is assumed to be one at the fire source and is diluted by entrained air to a value less then one as the gas flows away from the fire. Using the values K_m = 7600 m^2/kg [6], ε = 0.02 [6], h_r = 1.0 MW/m^2, h = 12 MJ/kg [11], v_L = 1.0 m/s, the above set of equations gives a value of S to be 0.0026 in order to obtain an optical density per meter of 3.3% m^{-1}. K_m, ε, and h are material dependent constants while h_r and v_l will depend on a number of variables including geometry. The requirement of knowing several material specific constants makes this method of smoke estimation difficult to use over the wide variety of fuel loads present in NASA facilities.

4.3 RADIATION DETECTION

Flaming fires radiate energy in the ultraviolet (UV), visible, and infrared (IR) portions of the electromagnetic spectrum. The quantity of radiation emitted in a particular spectral range depends on the type of fuel burning. For hydrocarbon fuels, the production of CO_2 produces a strong emission peak at about 4.3 μm. The production of large quantities of soot increases the amount of continuous emission radiated in the infrared and visible spectrum.

Many varieties of radiation detectors are available. Some IR detectors use filters to limit the detector sensitivity to a wavelength region near the CO_2 emission feature at 4.3 μm while other IR detectors are sensitive to a broadband of wavelengths in the infrared and visible portions of the spectrum. UV detectors are typically filtered to exclude sunlight and sodium or mercury emission from lights, and hence observe in a region from about 0.18 μm to 0.24 μm. In order to minimize false alarms, radiation detectors can be packaged with a combination of UV and IR sensors such that a non-fire source of either UV or IR radiation will not set off the detection system.

The CO_2 emission from burning hydrocarbon fuels can substantially increase the amount of IR radiation in the 4.1 μm to 4.7 μm band over what is expected in this spectral region from simply black-body radiation. The emission produced by non carbon containing fuels (eg, Mg, NH_3, H_2) generally will not contain this emission feature, but may generate other IR emission bands. Emission from electronic transitions of the combustion products determines the ultimate amount of UV radiation present. Recommendations concerning the use of radiation detectors must take into account the type of fuel hazard that is present. In some instances, broadband detectors in the visible and IR may be more appropriate for fire detection in special fuel situations than the standard detectors which take advantage of the strong infrared CO_2 emission feature.

5 MODELING RESULTS

5.1 Smoke and Heat Modeling

5.1.1 18 m to 24 m (60 ft to 80 ft)

One hypothetical geometry modeled was a 21 m (70 ft) high flat roof facility. The floor area was assumed to be 36 m by 36 m (120 ft by 120 ft). Simulated t-squared fires, reaching maximum heat release rates of 50 kW, 0.5 MW, 1.0 MW, 4.0 MW, and 50 MW in 100 s, were located on the floor at the center of the facility. It was assumed that air flowed into the facility through parallel rows of supplies located at the ceiling. Returns were located on the walls roughly 1.0 m (3 ft) above the floor. Air flows leaving the supplies were studied for flow velocities of 0.25 m/s and 1.0 m/s.

The results of these calculations are presented in table 1. An example of the temperature contours in the plane of the fire produced by a 1 MW fire at 90 s is displayed in Figure 1. Only the left half of the fire is shown in the figure. Note that the vent flow at the ceiling above the center of the fire reduces the temperature at the ceiling. For weak plumes such as this one, ceiling vents produce a measurable effect on the local temperature of the gas. Based on all the calculations for the cases in table 1, the following conclusions may be drawn about detector activation.

- Ceiling mounted fusible links designed to activate at temperatures of 57 °C (135 °F) or higher would not activate for test fires of 4 MW or less. Fusible links designed to activate at temperatures below 100 °C (212 °F) would be expected to activate for 50 MW fires in 90 s.

- Ceiling mounted rate-of-rise detectors will not activate for the test fires of 1 MW or less due to low ceiling temperatures. Ceiling mounted rate-of-rise detectors will activate for fires equal to or greater than 4 MW based on the observed ceiling temperature increase of 20 °C or more.

- Ceiling mounted smoke detectors would not be expected to activate for fires of less then 0.5 MW based on the ceiling temperatures not increasing above ambient. Smoke detectors operating at obscuration levels of 3.3% m^{-1} (1% ft^{-1}) (which lead to the 5 °C criterion) should activate for 4 MW and larger fires.

- Vent flows of 1 m/s lowered ceiling temperatures by roughly 10 °C in the 4 MW case. This decrease in temperature would not prevent the rate of rise and smoke detectors from activating but would bring the detection levels closer to the threshold values of the detectors.

5.1.2 24 m to 30 m (80 ft to 100 ft)

Two existing NASA facilities were modeled in this height range. The first facility is an orbiter processing and fueling facility, high bay designation KSC K6-696. This facility is 29 m (95 ft) high and has floor dimensions of 46 m by 60 m (150 ft by 197 ft). The facility contains a complex workstand which was designed to provide access to an orbiter. This facility is a clean room with an air flow of 2500 m^3/min (88000 cfm) introduced through supplies at the ceiling. Returns are located on the walls at a height of approximately 1.0 m (3 ft).

The bottom of the orbiter represents an impervious blockage of smoke and covers a substantial area. To investigate this effect, two blockages of different size were modeled using a 4 MW fire as shown in Figures 2 and 3. The blockage shown in Figure 2 is rectangular in shape with the length displayed in the figure equal to 6 m (20 ft). The blockage shown in Figure 3 is also rectangular, but the displayed length is increased to 16 m (52 ft). The increased area used in Figure 3 retards the smoke from reaching the ceiling. The blockage effect is enhanced by the location of the returns at the side walls which tend to prevent the weak plume from rising to the ceiling.

The second facility is an aircraft hangar (B1244) located at Langley Research Center. Based on the NASA survey, it was thought that this facility was 25 m (83 ft) high but after inspecting the construction plans, it was found that the structure is 28 m (93 ft) high. The roof of this facility was made up of several curved segments with the low point at the wall being 15 m (48 ft) high. The roof is level in the direction perpendicular to the curve. The floor of the hangar is 50 m by 43 m (160 ft by 140 ft) in area.

Temperature contours and velocity profiles are shown in Figures 4, 5, and 6 at 90 s for a 4 MW fire. The effect on the smoke movement for the down sloping side of the hangar roof is to slow the smoke flow compared with the flow along the level portion of the ceiling. The sloping ceiling impedes the smoke movement downslope, but accelerates smoke movement upslope.

The results of these calculations are presented in table 2a and 2b. Based on these results, the following conclusions may be drawn about detector activation.

> Ceiling mounted fusible links designed to activate at temperatures of 57 C (135 F) or higher would not activate for test fires of 4 MW or less within 90 s. Fusible links designed to activate at temperatures below 100 °C (212 °F) would be expected to activate for 50 MW fires in 90 s.

- Ceiling mounted rate-of-rise detectors would not activate for test fires of 1 MW or less due to low ceiling temperatures. Ceiling mounted rate-of-rise detectors would marginally activate for fires equal to 4 MW based on ceiling temperature increases of 15 °C. Ceiling mounted rate-of-rise detectors would activate for fires larger than 4 MW.

- Ceiling mounted smoke detectors would not be expected to activate for fires of 1 MW or less based on the ceiling temperatures not increasing above ambient. Smoke detectors operating at obscuration levels of 3.3% m^{-1} (1% ft^{-1}) which lead to the 5 °C criterion should activate for the 4 MW and larger fires.

For facilities, where a solid, nonflammable object as large as the orbiter is present, temperatures at the ceiling will be substantially lower compared with those produced by a freely rising plume if the smoke plume must travel significant horizontal distances before rising to the ceiling. Calculations for these cases assumed that the fire was located centered under the orbiter. Based on the results of the calculations for this fire placement, the following observations can be made. Rate-of-rise detectors will not activate for 4 MW and smaller fires. Fusible links designed to activate at temperatures of 57 °C (135 °F) or higher will not activate for 50 MW and smaller fires due to decreased ceiling temperatures. Smoke detectors operating at obscuration levels leading to the 5 °C criterion will not activate for fires of 4 MW or less due to low ceiling temperatures.

5.1.3 30 m to 36 m (100 ft to 120 ft)

Two geometries were modeled at this height. The first is a NASA orbiter payload processing/fueling structure, KSC M7-1469. This structure is a clean room with a 32 m (105 ft) high ceiling and is 46 m by 23 m (150 ft by 75 ft) in floor area. Supplies are located on the ceiling with returns located on the sidewalls of the facility. The ventilation system supports two to four air changes per hour. An interesting feature in this structure is the workstand used to support and service orbiter payloads. While a coarse grid of 49000 cells was used to model half the facility using a symmetry plane down the center of the building, a 21000 cell grid was used to model just the workstands in a second calculation set. The purpose of the detailed workstand grid was to investigate the possible impact that the workstand could produce on the smoke movement within the building.

An example of the geometry used to approximate the work stand is given in Figure 7. The rectangular solid located in the back center of the structure is a simulated orbiter payload. The four deck-like structures represent four working floors of the workstand. The working floors are steel grates but were modeled as

solids in this work. The actual situation is a complicated combination of grates and blockages as there are significant amounts of equipment positioned on each of the floors.

The effects of a 4 MW growing fire at 100 s is shown in Figure 8 where the arrows depict the direction and magnitude of the flow while the color of the arrows indicates the velocity. Note the shadowing effect that the orbiter payload has on the flow. Entrainment of air into the plume occurs at all levels of the workstand.

The second geometry is a 37 m (120 ft) high structure with a 18 m by 18 m (120 ft by 120 ft) floor area. Supplies are located on the ceiling with returns located on the sidewalls of the facility.

The t-squared fires modeled in this height range consisted of 50 kW, and 1 MW, 4 MW and 50 MW fires which reached their peak heat release rate in 100 s. Shown in Figure 9 are the temperature contours resulting from a 4 MW fire at 90 s. There was no vent flow for this case. The results of the calculations for these spaces are presented in tables 3a and 3b. Based on these results, the following conclusions may be drawn concerning detector activation.

- Ceiling mounted fusible links designed to activate at temperatures of 57 °C (135 °F) or higher would not activate for test fires of 4 MW or less. Fusible links designed to activate at temperatures below 100 °C (212 °F) would be expected to activate for 50 MW fires in 90 s as long as negligible air flow is present. For air flows of 1 m/s or greater, fusible links will not activate within 100 s for 50 MW fires.

- Ceiling mounted rate-of-rise detectors will not activate for test fires of 4 MW or less due to ceiling temperatures not rising more than 10 °C at the ceiling. Ceiling mounted rate-of-rise detectors will not activate for fires of 4 MW or less. The threshold for activation of these detectors at this height is not determined in this study.

- Ceiling mounted smoke detectors would not be expected to activate for fires of 1 MW or less based on the ceiling temperatures not increasing above ambient. Smoke detectors operating at obscuration levels of 3.3% m^{-1} (1% ft^{-1}) which lead to the 5 °C criterion should activate for the 4 MW fire size with no forced ventilation but will not activate within 100 s when 1 m/s ceiling flows are present.

5.2 RADIATION MODELING

Radiation detectors used at present NASA sites are primarily UV/IR with an activation criterion of being able to detect a 0.3 m by 0.3

m (1 ft by 1 ft) hydrocarbon fire at 14 m (45 ft). The heat release rate for a 0.3 m by 0.3 m (1 ft by 1 ft) gasoline fire is 110 kW. Gasoline fires are one of the common hydrocarbon fuels used to test the sensitivity of UV/IR detectors. Using RADTECT, the total infrared flux from a conical flame incident on a vertical surface at 13.7 m (45. ft) is 31 W/m^2 for a fuel with a radiation fraction of 35%. For fires with a heat release rate of 50 kW, in order to receive the same total infrared flux, detectors would have to be positioned no more than 9 m (30 ft) from the fire source.

6 SUMMARY

Based on the fire modeling discussed above, expected detector activation as a function of fire size can be summarized in tabular form for high bay facilities. Tables 4, 5, and 6 provide guidelines for expected activation of heat and smoke detectors as a function of ceiling height, forced ventilation, and fire size. A "Y" in a particular column means that for the given height and fire size, a particular detector should activate. A "N" in a particular column means that the detector would not be expected to activate.

The columns providing ceiling temperature and maximum target link temperature require additional explanation. A number of calculations were run for 90 s rather than the full 100 s growth of the fire. The ceiling temperatures for these runs are marked with an asterisk. Occasionally, a calculation of ceiling temperature will not have been made for a particular case and is designated as "NC" for not calculated. The column specifying target link temperatures represents an estimate of the maximum link temperature which would activate for a given fire. This estimate is based on a temperature which is 10 °C lower than the ceiling temperature reached at 100 s, or it is equal to the 90 s ceiling temperature for those calculations which were done only for 90 s. For cases where the ceiling temperature is too low, no link temperature is given.

The time of activation will depend on the growth rate of the fire with many fires requiring time periods longer than the 100 second period used for these calculations to reach full involvement. For rate of rise detectors, a slowly growing fire may not produce activation even though activation is indicated in the tables since these detectors depend both on temperature and rate of temperature rise. For slowly growing fires, the temperature rise requirement may not be realized.

As discussed earlier, large lateral blockages, which completely halt the vertical rise of the fire plume, can have a significant impact on the temperature and location of the plume at the ceiling as well as the time required for the hot smoke to reach the ceiling. When large lateral blockages are present, detectors must be sited underneath the blockages for fire detection purposes. If

the height from the floor to the blockage is greater than 18 m (60 ft), the guidelines for detector type contained in this paper should be used.

The detection of hydrocarbon fires with a heat release rate of 50 kW using UV/IR detectors requires more sensitive detectors than are now used for current NASA facilities. Based on infrared emission, present NASA installations should be able to see a 50 kW hydrocarbon fire 9 m (30 ft) from the detector. Since UV emission will also decrease as the target detectable hydrocarbon fire size is decreased from 110 kW to 50 kW, detector manufacturers should be consulted concerning the sensitivity of their detectors to these small fire sizes. The use of more sensitive detectors may require additional effort in order to avoid false alarms from nonfire sources.

The guidelines on detector activation discussed above are based on computer models of fire. Actual fire growth may deviate substantially from the fire growth assumed in the models. When using these guidelines for detection design, expected fire growth, ventilation, and building geometry must be taken into account to insure that the modeling assumptions are consistent with the design application.

REFERENCES

[1] NFPA 72E, Standard on Automatic Fire detectors, National Fire Protection Association, Quincy, MA., 1987.

[2] HARWELL FLOW3D, Release 3.2: User Manual, CFD Department, AEA Industrial Technology, Harwell Laboratory, Oxfordshire, United Kingdom. October, 1992.

[3] Launder, B. E. and Spalding, D. B., The numerical computation of turbulent flows, Computer Methods in Applied Mechanics and Engineering 3, 1974, p.269 - 289.

[4] Notarianni, K. A. and Davis, W. D., The Use of Computer Models to Predict Temperature and Smoke Movement in High Bay Spaces, National Institute of Standards and Technology, NISTIR 5304, December, 1993.

[5] Heskestad, G. and Smith, H. F., Investigation of a new sprinkler sensitivity approval test: The plunge test. Technical Report Serial No. 22485 2937, Factory Mutual Research Corporation, Norwood, MA., 1976. RC76-T-50.

[6] Mulholland, G. W., The SFPE Handbook of Fire Protection Engineering, Society of Fire Protection Engineering, Boston, MA, First Ed., 1988, p. 368-377.

[7] Evans, D. D., and Stroup, D. W., Methods to Calculate the Response Time of Heat and Smoke Detectors Installed below Large Unobstructed Ceilings. Fire Technology, Vol 22, No 1, February 1985 p. 54-63.

[8] Heskestad, G., and Delichatsios, M. A., Environments of Fire Detectors Phase 1; Effects of Fire Size, Ceiling Height and Material, Volume II - Analysis. Technical Report Serial No. 22427, RC 77-T-11. Factory Mutual Research Corporation, Norwood, MA., 1977.

[9] Notarianni, K. A., Measurement of Room Conditions and Response of Sprinklers and Smoke Detectors During a Simulated Two-Bed Hospital Patient Room Fire. National Institute of Standards and Technology, NISTIR 5240; July, 1993.

[10] Notarianni, K. A., Gott, J., Lowe, D., Davis, W. D., and Laramee, S., Analysis of High Bay Hangar Facilities for Detector Sensitivity and Placement. National Institute of Standards and Technology, NISTIR xxxx; 1996.

[11] Babrauskas, V., The SFPE Handbook of Fire Protection Engineering, Boston, MA, First Ed., 1988, p. 1- 15.

TABLE 1

Tabulated below are some of the initial conditions and results for the 21 meter (70 ft) facility. Descriptions for the column heading are as follows:

1. FIRE SIZE refers to the maximum heat release rate for the fire,
2. VENT FLOW refers to the speed of air flow out of a ceiling vent,
3. # GRID VOLUMES refers to the number of computational volumes used to represent a structure,
4. CEILING TEMP and CEILING SMOKE DENSITY are the temperature and smoke density calculated at plume center at time TIME after the start of the fire. Ambient temperature is 20 °C.
5. NC means not calculated in that run.
6. TIME is the elapsed time after the start of the simulated fire that corresponds with the temperature and smoke density values in the table.

FIRE SIZE MW	VENT FLOW m/s	# GRID VOLUMES	CEILING TEMP °C	CEILING SMOKE DENSITY	TIME s
0.05	0.0	19000	22	0.001	100
0.05	1.0	19000	20	0.0	100
0.5	0.0	17575	27	0.003	90
0.5	1.0	17575	21	0.002	90
0.5	0.25	19000	21	0.002	90
0.5	1.0	19000	21	0.002	90
1.0	1.0	19000	22	0.003	90
4.0	0.0	17575	45	NC	100
4.0	0.25	17575	37	NC	90
4.0	1.0	17575	36	NC	90
50.	1.0	17575	154	0.004	90

Table 2a

Tabulated below are some of the initial conditions and results for the NASA orbiter facility. Descriptions for the column heading are as follows:

1. FIRE SIZE refers to the maximum heat release rate for the fire,
2. VENT FLOW refers to the speed of air flow out of a ceiling vent,
3. # GRID VOLUMES refers to the number of computational volumes used to represent a structure,
4. CEILING TEMP is the temperature calculated at plume center at time TIME after the start of the fire. Ambient temperature is 20 °C.
5. Block refers to the 6 m or 16 m blockage described in the text. AB means fire was positioned above the blockage.
6. TIME is the elapsed time after the start of the simulated fire that corresponds with the temperature and smoke density values in the table.

FIRE SIZE MW	VENT FLOW m/s	# GRID VOLUMES	CEILING TEMP °C	block	TIME s
4.0	0.25	23064	34	6 m	100
4.0	0.25	23064	34	6 m	100
4.0	0.25	23064	34	6 m	200
50.	0.25	23064	92	6 m	100
50.	0.25	23064	102	6 m	200
50.	0.25	23064	47	16 m	100
50.	0.25	23064	82	16 m	200
4.0	0.25	23064	20	16 m	100
4.0	2.5	23064	20	16 m	100
4.0	1.0	23064	20	16 m	100
4.0	1.0	23064	20	16 m	200
4.0	1.0	23064	20	16 m	100
4.0	1.0	30504	37	AB	100
4.0	1.0	30504	20	16 m	100
4.0	1.0	30504	20	16 m	100

Table 2b

Tabulated below are some of the initial conditions and results for the Langley hangar. Descriptions for the column heading are as follows:

1. FIRE SIZE refers to the maximum heat release rate for the fire,
2. VENT FLOW refers to the speed of air flow out of a ceiling vent,
3. # GRID VOLUMES refers to the number of computational volumes used to represent a structure,
4. CEILING TEMP and CEILING SMOKE DENSITY are the temperature and smoke density calculated at plume center at time TIME after the start of the fire.
5. NC means not calculated in that run.
6. TIME is the elapsed time after the start of the simulated fire that corresponds with the temperature and smoke density values in the table.

FIRE SIZE MW	VENT FLOW m/s	# GRID VOLUMES	CEILING TEMP °C	CEILING SMOKE DENSITY	TIME s
4.0	0.0	30600	25	NC	90
4.0	0.0	30600	37	NC	180

Table 3a

Tabulated below are some of the initial conditions and results for the NASA payload facility. Descriptions for the column heading are as follows:

1. FIRE SIZE refers to the maximum heat release rate for the fire,
2. VENT FLOW refers to the speed of airflow out of a ceiling vent,
3. # GRID VOLUMES refers to the number of computational volumes used to represent a structure,
4. CEILING TEMP and CEILING SMOKE DENSITY are the temperature and smoke density calculated at plume center at time TIME after the start of the fire.
5. NC means not calculated in that run.
6. TIME is the elapsed time after the start of the simulated fire that corresponds with the temperature and smoke density values in the table.

FIRE SIZE MW	VENT FLOW m/s	# GRID VOLUMES	CEILING TEMP °C	CEILING SMOKE DENSITY	TIME s
1.0	0.0	49152	25	NC	75
4.0	1.0	49152	42	NC	100
4.0	0.0	49152	36	NC	75
4.0	0.25	20790	34	0.008	100

Table 3b

Tabulated below are some of the initial conditions and results for the 37 m (120 ft) facility. Descriptions for the column heading are as follows:

1. FIRE SIZE refers to the maximum heat release rate for the fire,
2. VENT FLOW refers to the speed of air flow out of a ceiling vent,
3. # GRID VOLUMES refers to the number of computational volumes used to represent a structure,
4. CEILING TEMP and CEILING SMOKE DENSITY are the temperature and smoke density calculated at plume center at time TIME after the start of the fire.
5. NC means not calculated in that run.
6. TIME is the elapsed time after the start of the simulated fire that corresponds with the temperature and smoke density values in the table.

FIRE SIZE MW	VENT FLOW m/s	# GRID VOLUMES	CEILING TEMP °C	CEILING SMOKE DENSITY	TIME s
1.0	0.0	13357	25	NC	90
4.0	0.0	13357	33	NC	90
50.	0.0	13357	109	NC	90
1.0	1.0	26011	20	NC	90
0.05	1.0	26011	20	0.0	90
4.0	1.0	26011	22	0.0005	60
50.	1.0	26011	41	0.004	60

Table 4

18 m to 24 m (60 ft to 80 ft)

Values in this table are for unobstructed spaces. Large lateral blockages may have a substantial impact on detection strategies.

Max. Fire Size (MW)	Forced Flow 1.0 m/s	Ceiling Temp (C) * means 90 s	Maximum Target Link Temp (C)	Smoke 2.5% m^{-1}	Rate of Rise 15 °C in 60 s
0.05	N	22		N	N
0.05	Y	20		N	N
0.5	N	27*		Y	N
0.5	Y	21*		Y	N
1.0	N	NC		Y	N
1.0	Y	22*		Y	N
4.0	N	45	37	Y	Y
4.0	Y	37*	37	Y	Y
50.0	N	NC	154	Y	Y
50.0	Y	154	154	Y	Y

Table 5

24 m to 30 m (80 ft to 100 ft)

Values in this table are for unobstructed spaces. Large lateral blockages may have a substantial impact on detection strategies.

Max. Fire Size (MW)	Forced Flow 1.0 m/s	Ceiling Temp (C)	Maximum Target Link Temp (C)	Smoke 2.5% m^{-1}	Rate of Rise 15 °C in 60 s
0.05	N	NC		N	N
0.05	Y	NC		N	N
1.0	N	NC		Y	N
1.0	Y	NC		Y	N
4.0	N	37		Y	N
4.0	Y	34		Y	N
50.0	N	NC	82	Y	Y
50.0	Y	92	82	Y	Y

Table 6

30 m to 36 m (100 ft to 120 ft)

Values in this table are for unobstructed spaces. Large lateral blockages may have a substantial impact on detection strategies.

Max. Fire Size (MW)	Forced Flow 1 m/s	Ceiling Temp (C) * means 90 s	Maximum Target Link Temp (C)	Smoke 2.5% m^{-1}	Rate of Rise 15 °C in 60 s
0.05	N	NC		N	N
0.05	Y	20*		N	N
1.0	N	25*		N	N
1.0	Y	20*		N	N
4.0	N	33*		Y	N
4.0	Y	NC		N	N
50.	N	109*	109	Y	Y
50.	Y	NC	109	Y	Y

APPENDIX A

HARWELL FLOW3D INPUTS

Table A.1

Turbulence Parameters

Input Variable	Value
C_1	1.44
C_2	1.92
C_3	1.00
C_μ	0.18
Prandtl Number For Enthalpy	0.85

Table A.1

Ceiling Material Constants

Constant	Value
Thermal Conductivity	60.0 W/(m K)
Specific Heat	480. J/(kg K)
Density	7850. kg/m^3

Table A.3

Model Physics

Turbulent Flow (k-ε Model)
Compressible Flow
Heat Transfer (Ceiling only)
Buoyant Flow
Transient Flow

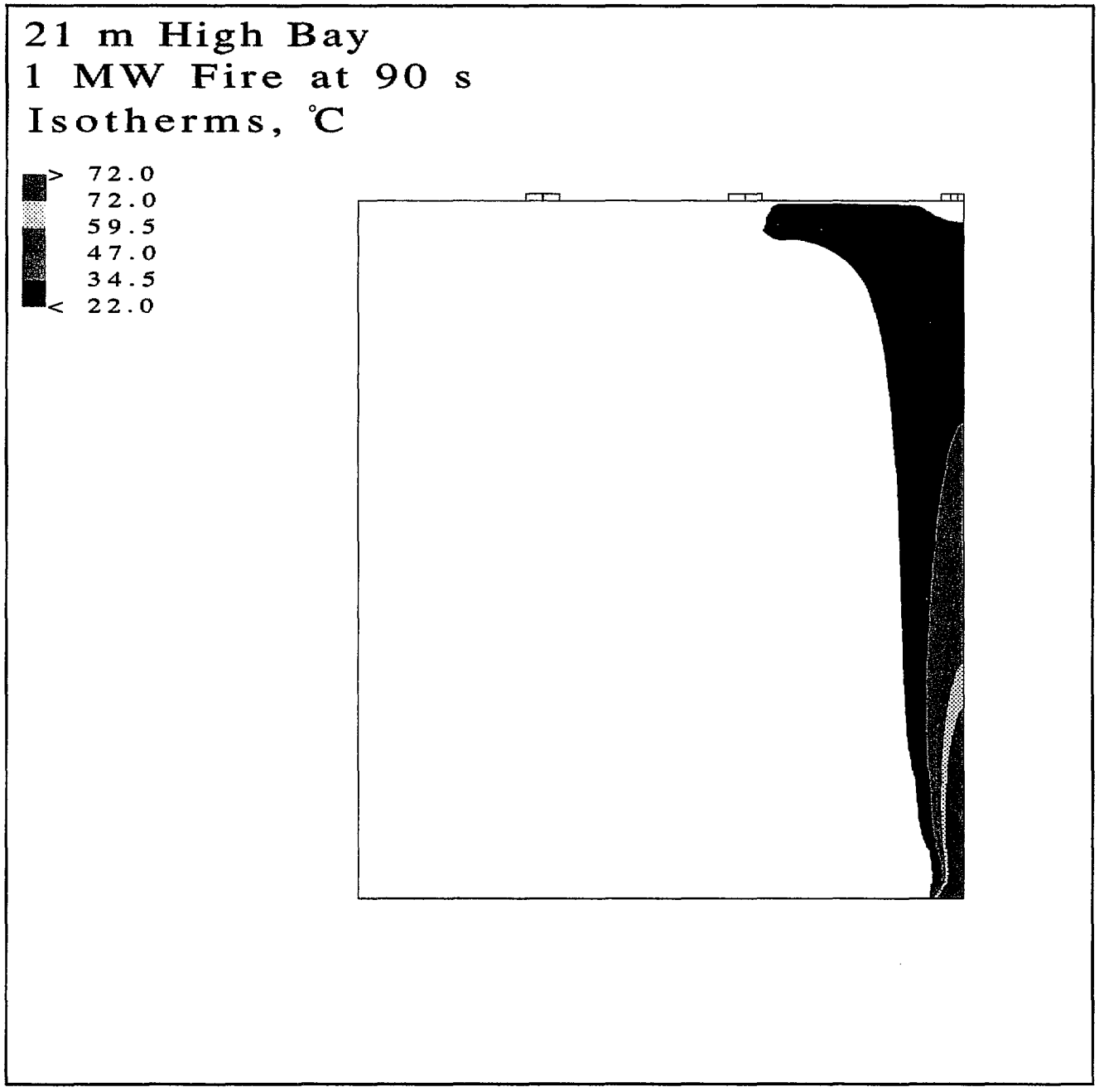

Figure 1: Temperature isotherms at 90 s for a 1 MW fire in a 21 m high bay.

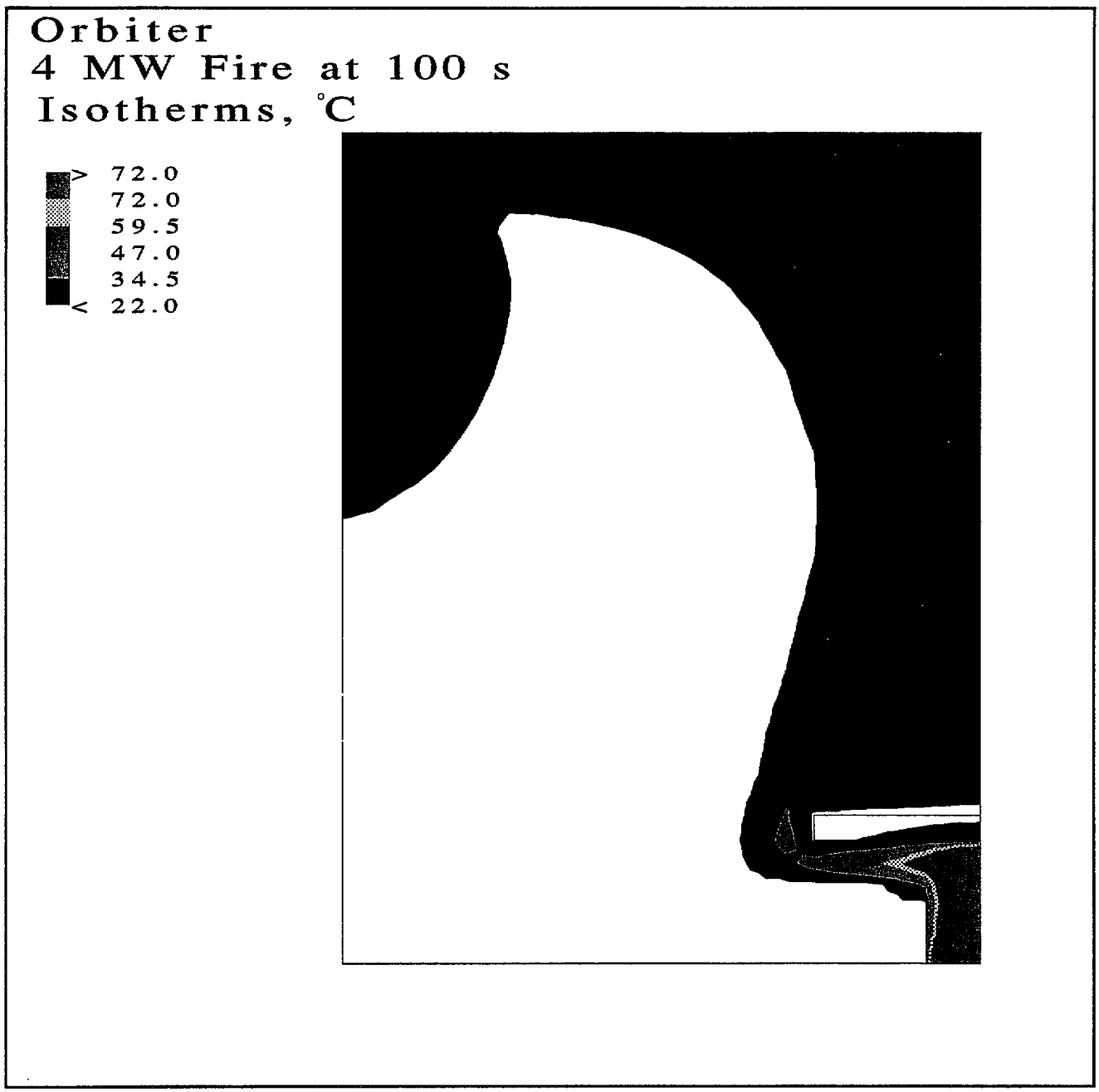

Figure 2: Temperature isotherms at 100 s for a 4 MW fire located under a 6m blockage in a 29 m high bay.

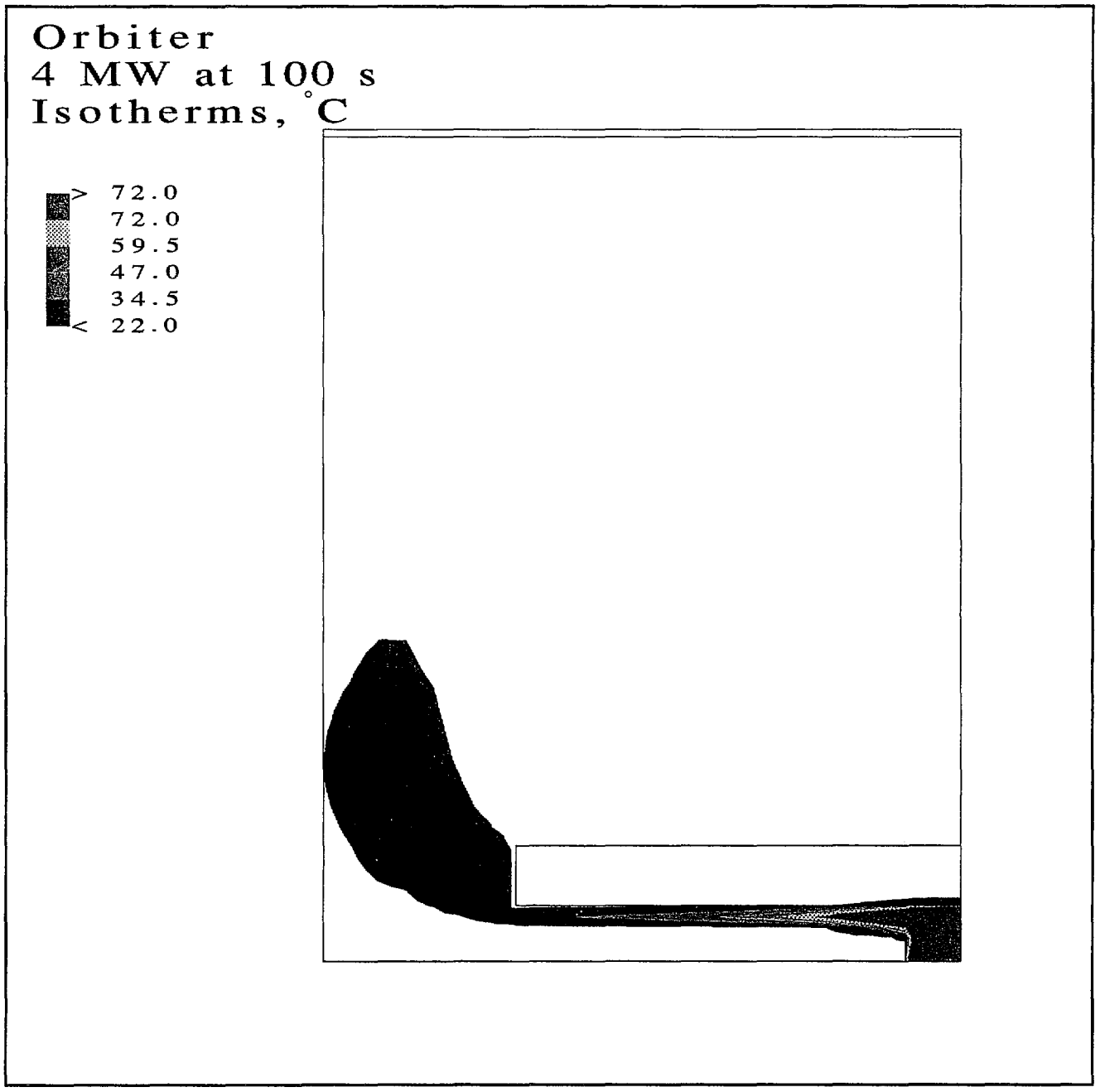

Figure 3: Temperature isotherms at 100 s for a 4 MW fire located under a 16 m blockage in a 29 m high bay.

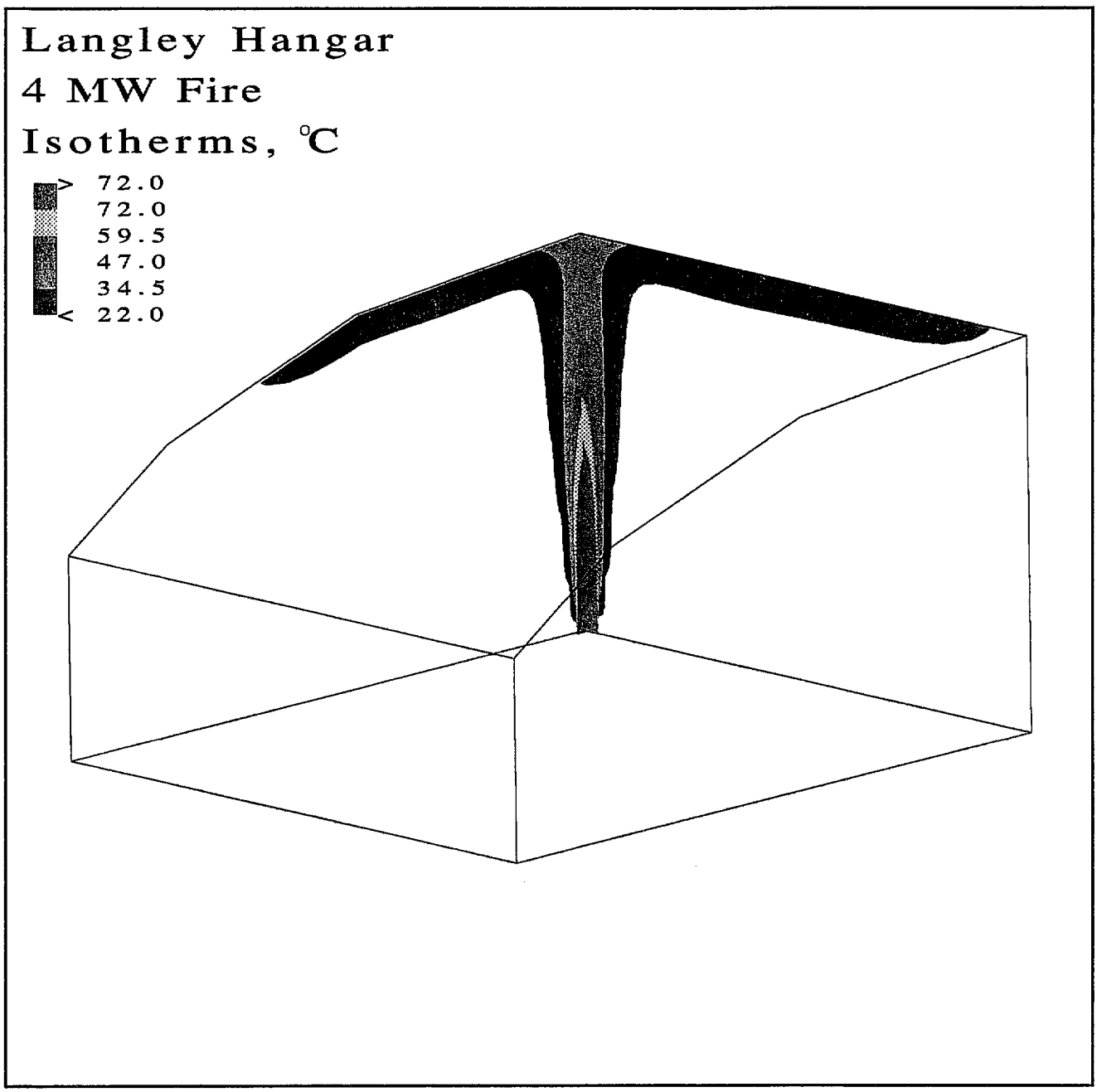

Figure 4: Temperature isotherms at 90 s for a 4 MW fire located in a 28 m high hangar.

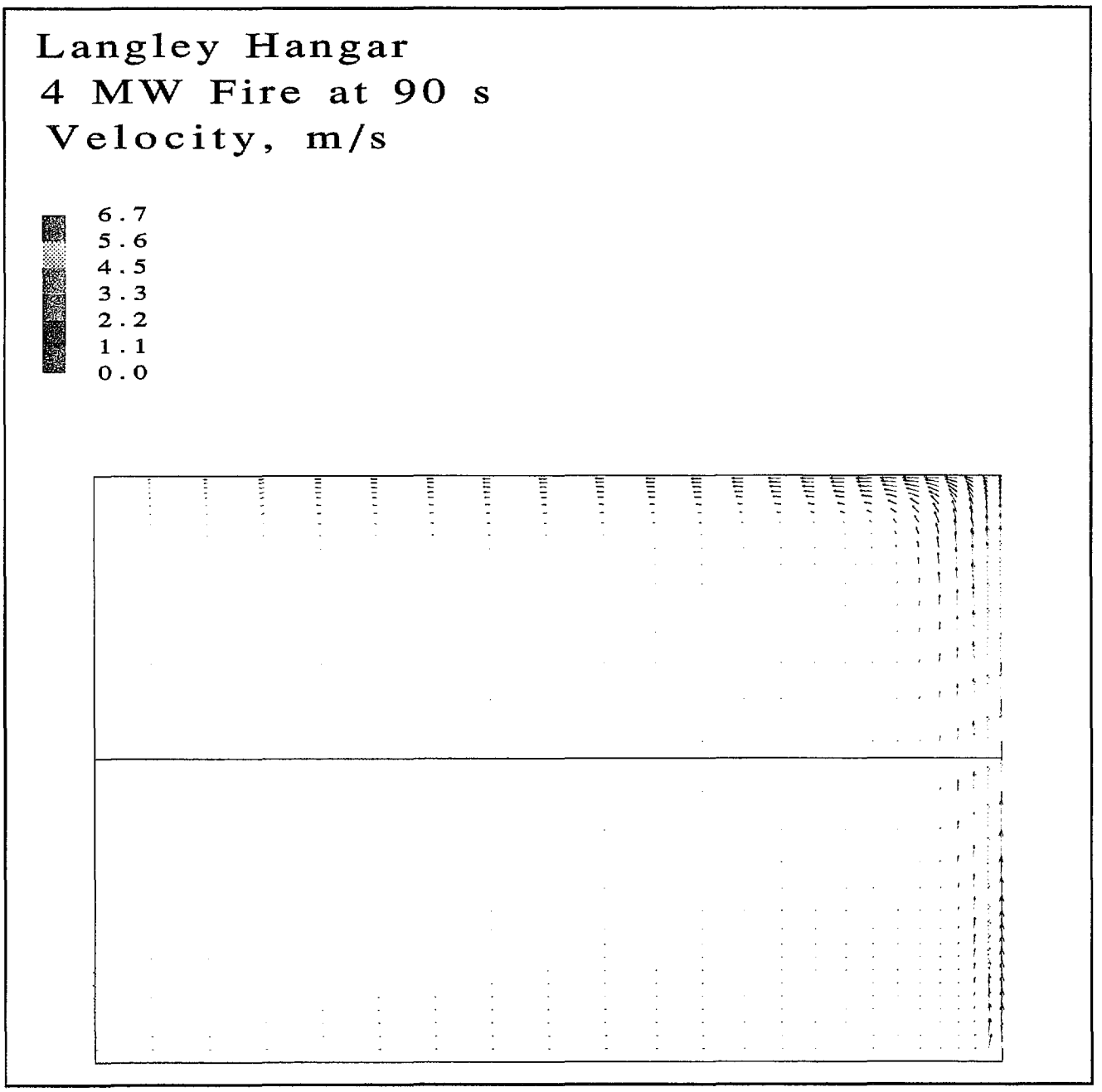

Figure 5: Velocity vectors representing the air flow at 90 s for a 4 MW fire displayed in a plane located at the center of the hangar with a ceiling height of 28 m.

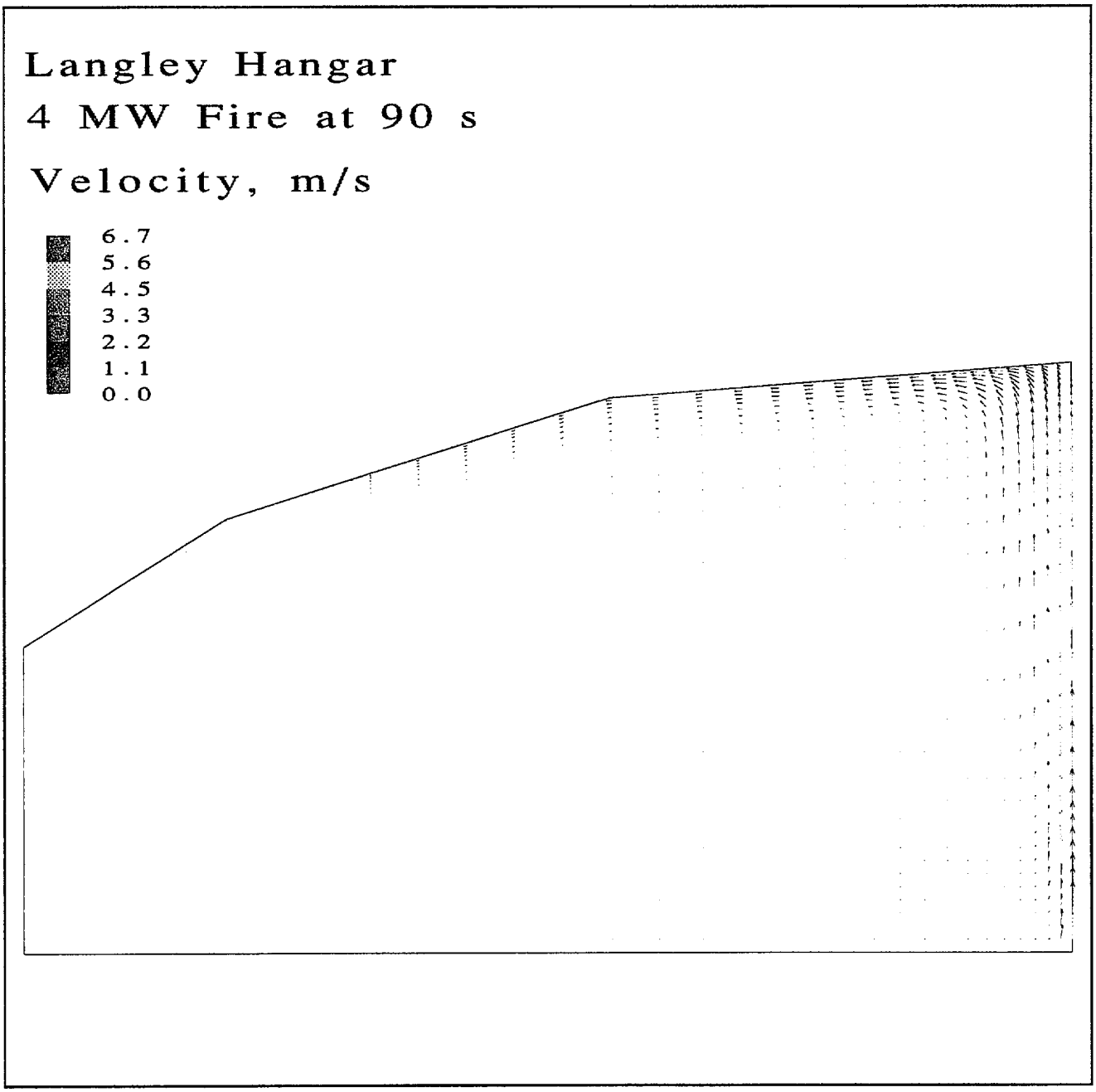

Figure 6: Velocity vectors representing the air flow at a 90 s for a 4 MW fire displayed in a plane located at the center of the hangar in the direction of decreasing ceiling height.

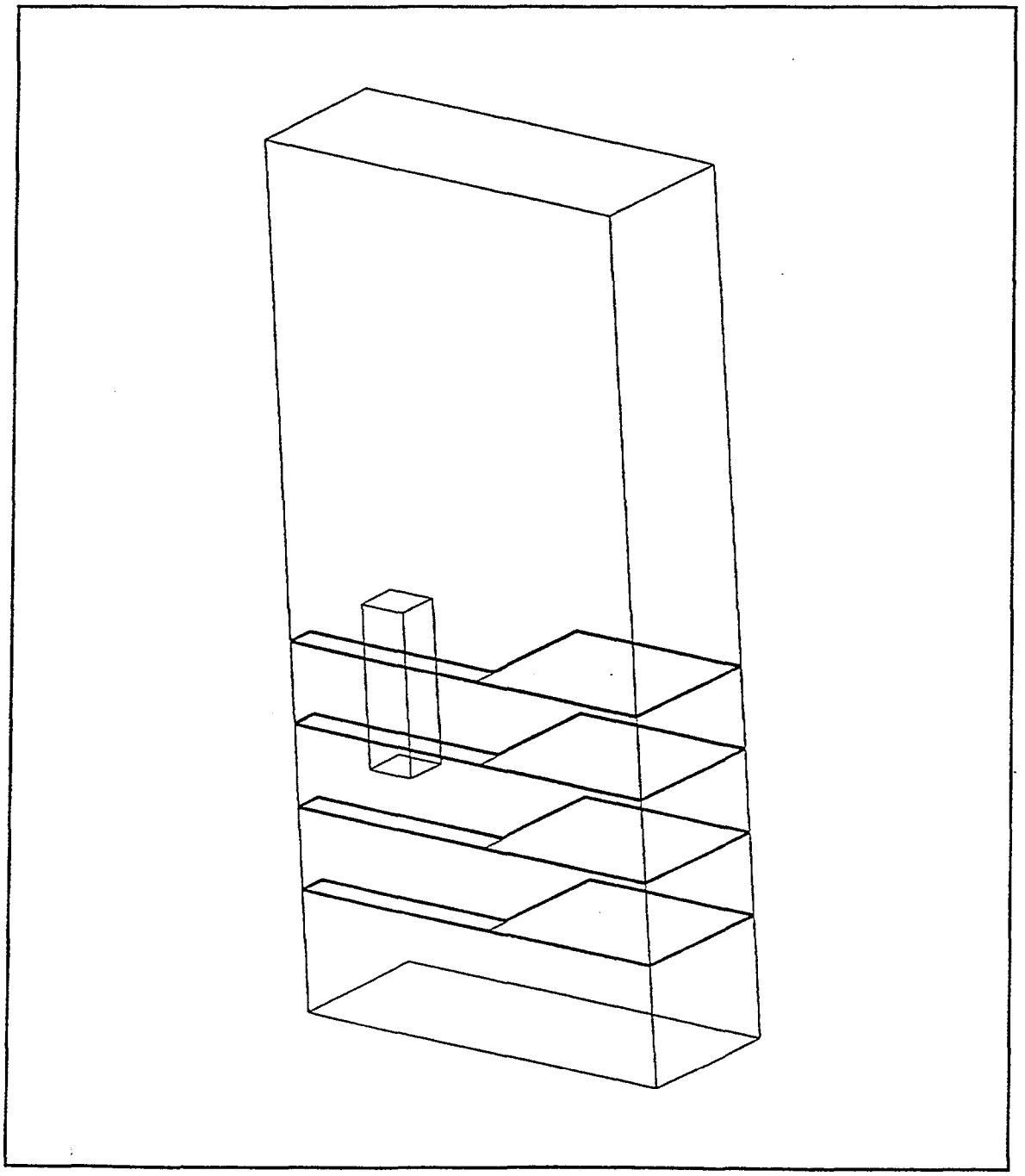

Figure 7: A representative geometry used to model the orbiter work stand. The flat rectangles represent iron gratings and are assumed to stop the air flow. The parallelepiped represents a paperload.

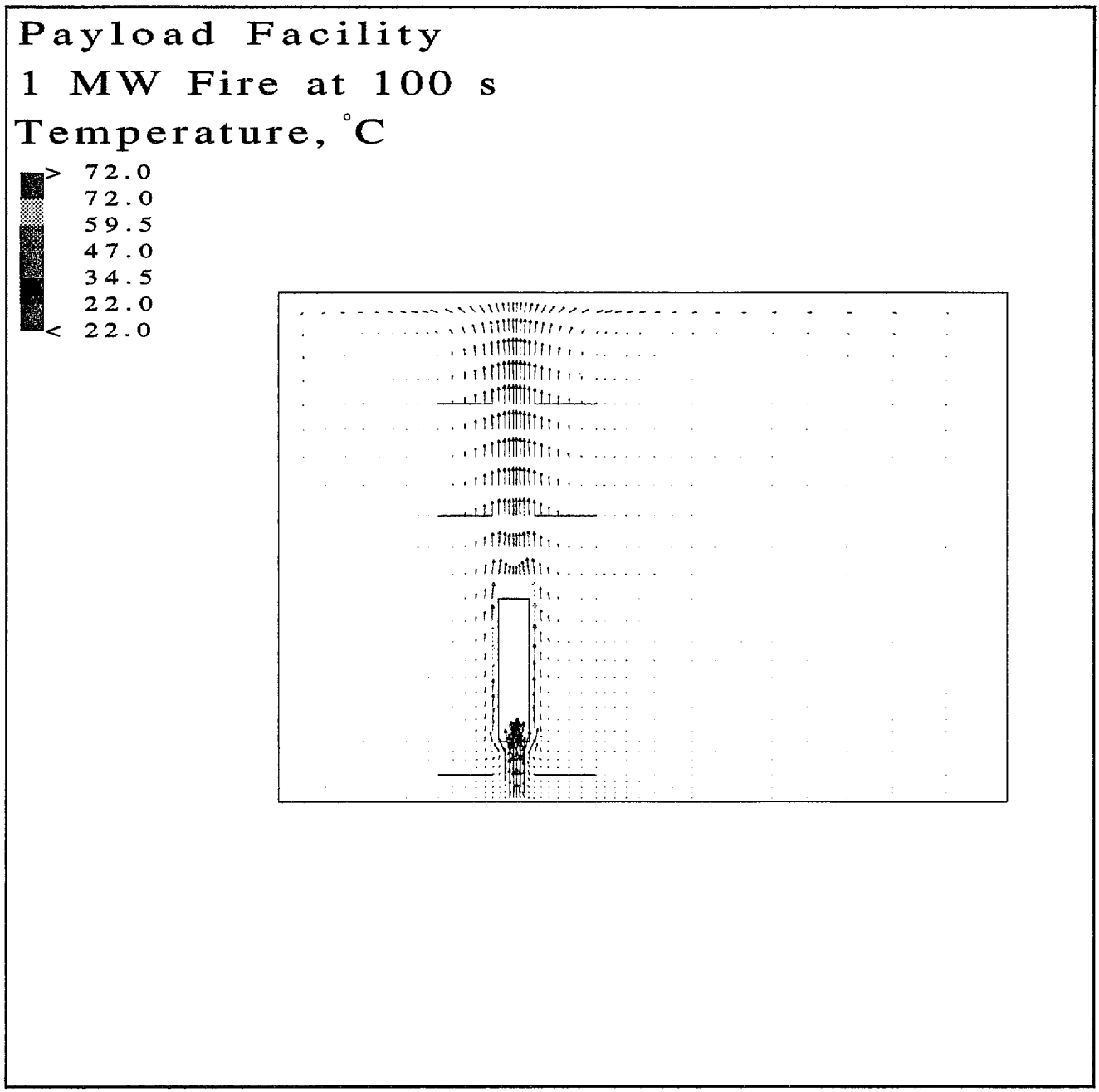

Figure 8: Velocity vectors representing the air flow at 100 s for a 1 MW fire underneath a orbiter payload.

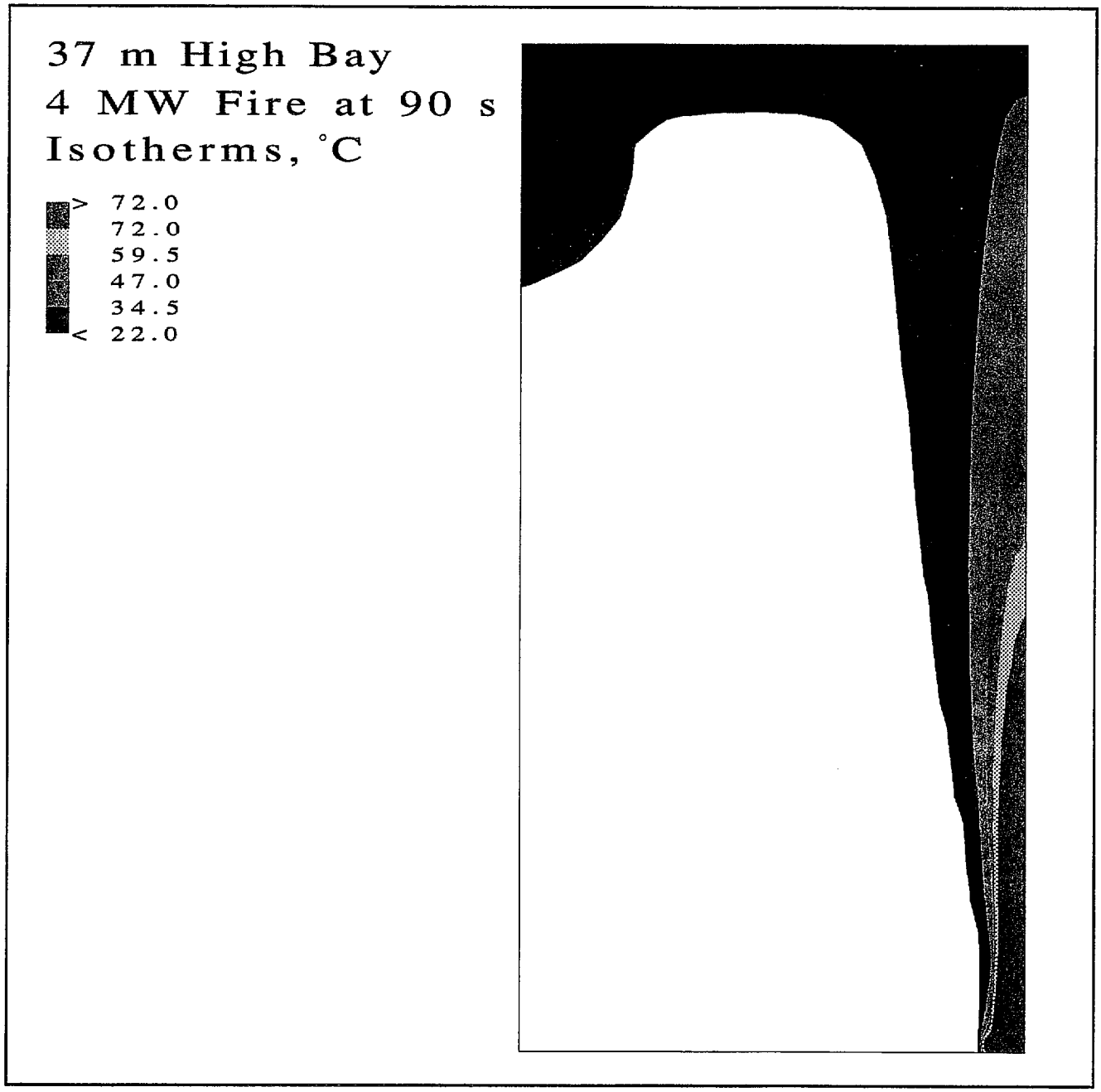

Figure 9: Temperature isotherms at 90 s for a 4 MW fire located in a 37 m high bay.

NIST-114
(REV. 6-93)
ADMAN 4.09

U.S. DEPARTMENT OF COMMERCE
NATIONAL INSTITUTE OF STANDARDS AND TECHNOLOGY

MANUSCRIPT REVIEW AND APPROVAL

(ERB USE ONLY)
ERB CONTROL NUMBER | DIVISION: 764
PUBLICATION REPORT NUMBER: NISTIR 5798 | CATEGORY CODE

INSTRUCTIONS: ATTACH ORIGINAL OF THIS FORM TO ONE (1) COPY OF MANUSCRIPT AND SEND TO THE SECRETARY, APPROPRIATE EDITORIAL REVIEW BOARD

PUBLICATION DATE: March 1996 | NUMBER PRINTED PAGES

TITLE AND SUBTITLE (CITE IN FULL)

NASA FIRE DETECTION STUDY

CONTRACT OR GRANT NUMBER

TYPE OF REPORT AND/OR PERIOD COVERED

AUTHOR(S) (LAST NAME, FIRST INITIAL, SECOND INITIAL)
Davis, William D. and Notarianni, Kathy A.

PERFORMING ORGANIZATION (CHECK (X) ONE BOX)
[x] NIST/GAITHERSBURG
[ ] NIST/BOULDER
[ ] JILA/BOULDER

LABORATORY AND DIVISION NAMES (FIRST NIST AUTHOR ONLY)
Building and Fire Research Laboratory, Fire Safety Engineering Division

SPONSORING ORGANIZATION NAME AND COMPLETE ADDRESS (STREET, CITY, STATE, ZIP)
National Aeronautics and Space Administration
NASA Headquarters
Office of Safety and Mission Assurance

PROPOSED FOR NIST PUBLICATION

[ ] JOURNAL OF RESEARCH (NIST JRES)	[ ] MONOGRAPH (NIST MN)	[ ] LETTER CIRCULAR
[ ] J. PHYS. & CHEM. REF. DATA (JPCRD)	[ ] NATL. STD. REF. DATA SERIES (NIST NSRDS)	[ ] BUILDING SCIENCE SERIES
[ ] HANDBOOK (NIST HB)	[ ] FEDERAL INF. PROCESS. STDS. (NIST FIPS)	[ ] PRODUCT STANDARDS
[ ] SPECIAL PUBLICATION (NIST SP)	[ ] LIST OF PUBLICATIONS (NIST LP)	[ ] OTHER _____
[ ] TECHNICAL NOTE (NIST TN)	[x] NIST INTERAGENCY/INTERNAL REPORT (NISTIR)	

PROPOSED FOR NON-NIST PUBLICATION (CITE FULLY) [x] U.S. [ ] FOREIGN

PUBLISHING MEDIUM
[x] PAPER [ ] CD-ROM
[ ] DISKETTE (SPECIFY) _____
[ ] OTHER (SPECIFY)

SUPPLEMENTARY NOTES

ABSTRACT (A 2000-CHARACTER OR LESS FACTUAL SUMMARY OF MOST SIGNIFICANT INFORMATION. IF DOCUMENT INCLUDES A SIGNIFICANT BIBLIOGRAPHY OR LITERATURE SURVEY, CITE IT HERE. SPELL OUT ACRONYMS ON FIRST REFERENCE.) (CONTINUE ON SEPARATE PAGE, IF NECESSARY.)

The National Aeronautics and Space Administration, together with the National Institute of Standards and Technology are in the third year of a five year project designed to set guidelines for fire protection in high bay facilities. A high bay facility is defined in this study as any space with a ceiling height in excess of 18 m. NASA has numerous high bay spaces that are used to perform a variety of functions. A survey of NASA high bay spaces was conducted to determine the number of spaces, the use of the space, fire detection and suppression present,geometry and presence of forced air flow or clean room conditions, and special hazards which would pose substantial fire risks. Based on the survey results, a modeling program was designed which would analyze both specific and generic high bay spaces representative of the NASA inventory. The computation fluid dynamics model HARWELL-FLOW3D was used for the modeling. The object of the modeling was to simulate the response of smoke, fusible link, heat, UV/IR, and obscuration detectors to several standard fire scenarios. The modeling was done for both force air flow and no air flow present in the space. Results of the predicted detector activation times are presented as a function of fire size, ceiling height, and forced air flow.

KEY WORDS (MAXIMUM OF 9; 28 CHARACTERS AND SPACES EACH; SEPARATE WITH SEMICOLONS; ALPHABETIC ORDER; CAPITALIZE ONLY PROPER NAMES)
fire simulation; fluid flow; heat detection; radiation detection;
smoke detection; ventilation; aircraft hangars; detection time; fire models

AVAILABILITY
[x] UNLIMITED [ ] FOR OFFICIAL DISTRIBUTION - DO NOT RELEASE TO NTIS
[ ] ORDER FROM SUPERINTENDENT OF DOCUMENTS, U.S. GPO, WASHINGTON, DC 20402
[x] ORDER FROM NTIS, SPRINGFIELD, VA 22161

NOTE TO AUTHOR(S): IF YOU DO NOT WISH THIS MANUSCRIPT ANNOUNCED BEFORE PUBLICATION, PLEASE CHECK HERE. [ ]

WORDPERFECT